Control of Plug-in Hybrid Electric Vehicles for Mobile Power Generation and Grid Support Applications

Gui-Jia Su and Lixin Tang
Energy and Transportation Science Division
Oak Ridge National Laboratory
Knoxville, U.S.A.
sugj@ornl.gov

***Abstract*—The use of an onboard electrical propulsion system in a hybrid electric vehicle (HEV) to provide plug-in charging, mobile power generation, and vehicle-to-grid support capabilities is discussed. Pulse width modulation (PWM) control methods are examined for operating such a plug-in HEV in mobile power generation and vehicle-to-grid support applications to assess their impacts on the power conversion efficiency. A novel unipolar/interleaved PWM switching scheme is proposed, which can significantly reduce the switching losses and substantially increase the efficiency. A dual inverter drive prototype was assembled to test the PWM control schemes and test results are included to verify the effectiveness of the proposed control scheme.**

I. INTRODUCTION

The success of gasoline–electric hybrid vehicles in the market has made it well recognized that using an electric drive to augment the internal combustion engine (ICE) can effectively reduce pollutant emissions and increase gas mileage [1][2]. In an HEV, while the ICE still plays a dominant role for propulsion, the electric motor drive enables downsizing the ICE, operating the engine in its optimal efficiency regions, capturing and reusing the kinetic energy obtained during braking, and switching off the engine when the vehicle is stopped at red lights or in traffic jams, thus boosting the fuel efficiency significantly. This improvement on fuel economy is especially effective in city driving, where vehicles are operated frequently in stop and start situations.

To further promote reductions of oil consumption and pollutant emissions by automobiles, interest has recently been increasing in research and development on plug-in HEVs (PHEVs), in which a larger battery pack is used so that it enables the vehicle to operate on the electric drive system alone, without running the ICE for a distance of several tens of kilometers (this is called charge-depletion or pure EV mode) [3]. The battery is charged by plugging into the grid; ideally done at home during night time to take the advantage of lower off-peak electricity rates. A PHEV thus operates first as a pure battery-electric vehicle and then switches to the conventional series HEV mode after the battery is discharged to a predefined level of state-of-charge. At that point, the ICE kicks in and operates as a generator to maintain the battery state-of-charge within a narrow band (charge sustaining mode). This type of HEV is specifically suitable for daily commutes within the electric drive ranges of the HEVs because no engine operations are needed over the entire commuting drive. Being capable of achieving zero emissions and substantially higher miles per gallon in the pure EV mode, PHEVs can reduce emissions and boost gas mileage more significantly than conventional HEVs [4].

Because both the size of the batteries for PHEVs and the amount of energy that can be stored in the batteries remain limited, to maximize the range for a PHEV in the EV mode, it is desired to charge the batteries whenever the vehicle is parked and as fast as they can be charged. Hence, an onboard charger with a high power rating is highly desirable. In addition, chargers with bidirectional power flow capability can enhance the functionality and value of the vehicles by providing additional capabilities. As the number of PHEVs continues to increase, these vehicles can collectively serve as a load leveling energy storage device to the grid; supplying power to the grid during peak demands and drawing power from the grid to charge the batteries during off-peak periods. This can also help facilitate the integration into the grid of renewable energy sources with an intermittent power generating nature such as wind and solar power plants. Moreover, a bidirectional charger can enable the vehicle to function as a mobile power generator. The requirements for this bidirectional charger are similar to those for other automotive parts—low cost, low volume and weight, and high efficiency and reliability. To reduce the cost of such a bidirectional charger, several methods of utilizing the onboard electrical propulsion system to fulfill the charging/power generating function are reported [5-9].

To maximize the fuel saving and emission reduction, the efficiency of the bidirectional charger needs to be enhanced. In this paper, pulse width modulation switching schemes uniquely suited for control of PHEVs that utilize onboard electrical propulsion inverters and motors for mobile power

generation and grid support applications are proposed and examined experimentally. In particular, it is found that a novel unipolar/interleaved PWM switching scheme can significantly reduce the switching losses and substantially increase the efficiency. A dual inverter drive prototype was assembled to test the PWM control schemes and experimental results are included to verify the effectiveness of the proposed control scheme.

II. System Description and Control

A. System Description

Fig. 1 shows a schematic of an HEV traction drive system configured for battery charging, mobile power generation, and grid support applications. The system consists of two motor/generators, MG1 and MG2, with MG2 coupled to the ICE, and two inverter/converters, INV/CONV1 and INV/CONV2. The basic idea is that by connecting the neutral points of the motors to the grid or external loads, the motor/generators can be used as inductors to eliminate the need for an extra external inductor and the two three-phase inverters can be operated as a single-phase ac-to-dc or dc-to-ac converter for charging the battery, feeding power to the grid or loads. Two sets of contact switches are used for safety and proper vehicle operation considerations; one for disconnecting the high-voltage (HV) battery pack from the drive system when the vehicle is not in operation and the other for disconnecting the charging socket and the filter capacitor, C_{acf}, when the vehicle is not operated in charging or generation modes. It is noted that the configuration shown in Fig. 1 is readily applicable to the series hybrid and power-split hybrid configurations. For the parallel hybrids, vehicle accessory drives such as the air-conditioning compressor drive can be used to replace INV/CONV1 and MG1.

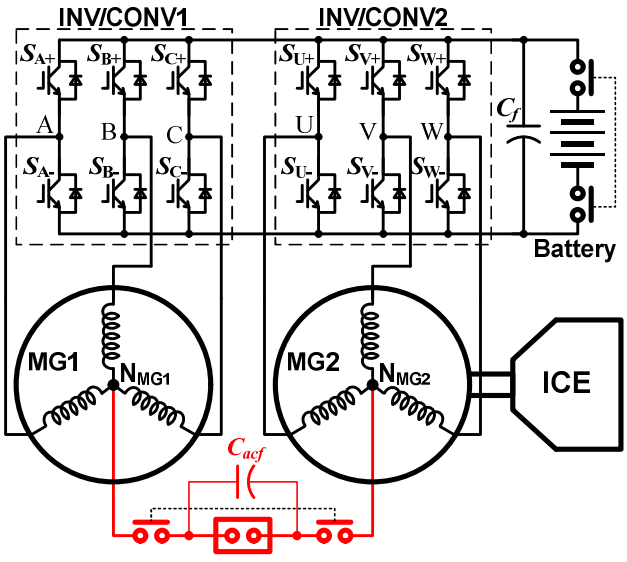

Figure 1. Schematic of utilizing the onboard traction drive system for battery charging, mobile power generation, and grid support applications.

All the switch legs in each inverter/converter collectively function as a single switch leg and the motor/generator as an inductor. Together, the two drive units form a single-phase converter/inverter to charge/discharge the battery, when operating in the grid support mode. When operating in the generation mode, the drive units form a single-phase inverter to supply the external loads. In this mode, the motor/generator (MG2) of the drive unit coupled to the engine shaft is driven by the engine to generate electrical power for supplying the dc bus and ultimately the external loads. Furthermore, power can be drawn from the HV battery for short time interval operations.

Fig. 2 shows an equivalent circuit of the electrical drive system for operating in the mobile generation mode, where electrical power is generated by MG2 that is driven by the engine. In this case, the three switch-legs in INV/CONV1 (A, B, and C) collectively function as the first single switch leg of the single-phase inverter and the MG1 as an impedance net work – its stator zero-sequence (ZS) impedance networks, ZSIN1. ZSIN1 consists of three identical branches and each branch is comprised of the stator winding phase resistance, R_{ms1}, and the phase leakage inductance, l_{m0s}. The other inverter/converter, INV/CONV2, has dual functions. It first operates as a three-phase converter to regulate the dc bus voltage, V_{dc}, by controlling the power generated by the generator, MG2. At the same time, its three phase-legs collectively form the second switch leg of the single-phase inverter to regulate the load voltage, v_{Load}. While the three-phase generator currents pass through its positive network and generate a breaking torque to the engine, the external load current splits into three equal parts and each part flows in one branch of its ZS network, ZSIN2, and as such does not produce air-gap flux or generate any torque.

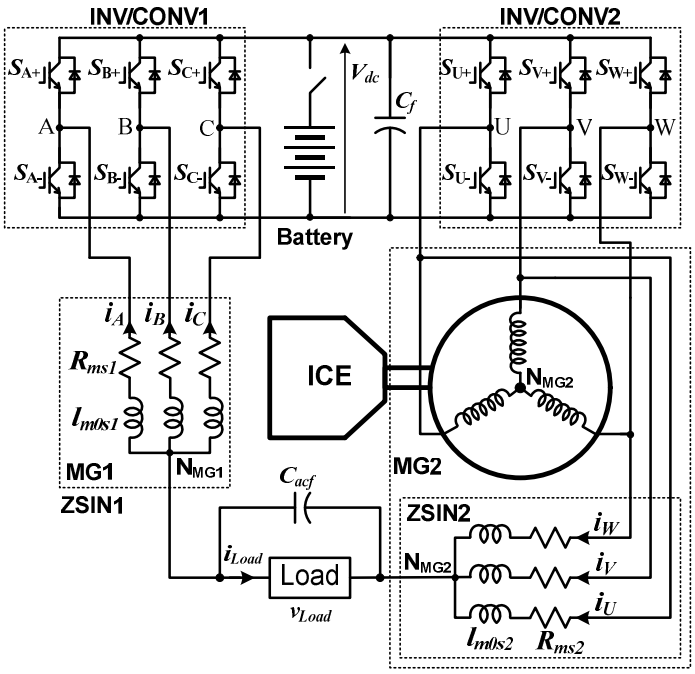

Figure 2. Equivalent circuit of the traction drive system for operating in the mobile power generation mode.

Fig. 3 shows an equivalent circuit of the electrical drive system for operating in the grid support mode. All the three switch-legs (A, B, and C or U, V, and W) in each of the two inverters/converters collectively function as a single switch leg and the motors/generators as two ZS impedance networks,

ZSIN1 and ZSIN2. Together, the two drive units form a single-phase converter to regulate the battery voltage, V_{bat}, or the charging current, I_{bat}, for charging the battery. Alternately, the two drive units form a single-phase inverter to discharge the battery to feed the grid for peak load support. Normally, the single-phase converter is controlled in such a way to maintain a unity power factor. It can also be used as a reactive power source for grid voltage support.

B. System Control

Fig. 4 shows control block diagrams for both the mobile power generation (a) and grid support operations (b). In (a), a field orientation based control is implemented for the generator, MG2, to maintain the dc bus voltage at a commanded level. The load voltage, v_{Load}, is controlled by the other inverter with a current control inner loop. In (b), the grid current is controlled by both inverters with the commanded current determined by grid demands and the battery charging/discharging profile.

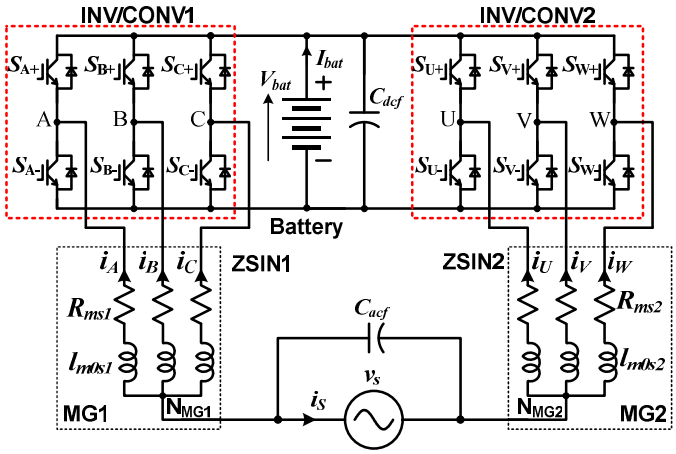

Figure 3. Equivalent circuit of the traction drive system for operating in vehicle-to-grid applications.

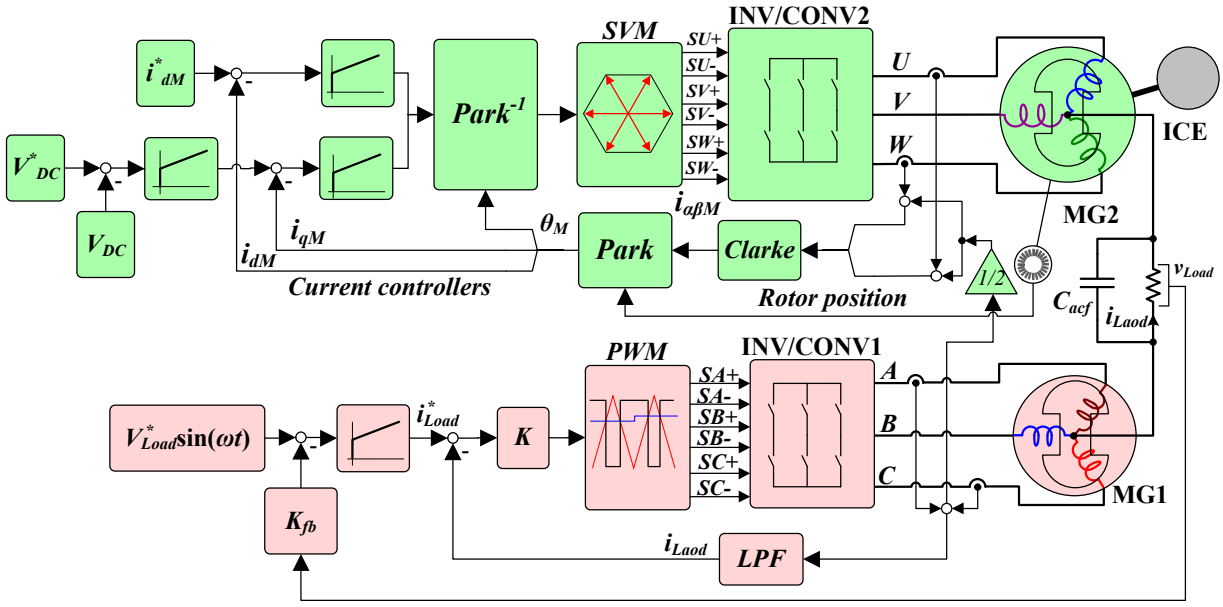

(a) For mobile power generation

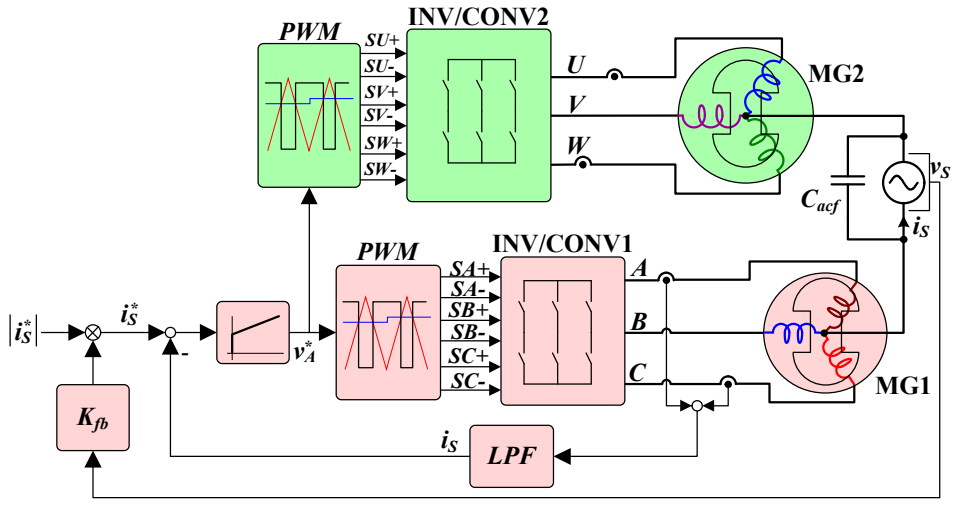

(b) For grid support

Figure 4. Control block diagrams.

Usually, only two phase currents (i_U and i_W or i_A and i_B in Fig. 3) of each motor/generator are sensed and fed back to the drive system controller for operating in the traction drive mode. Assuming each stator phase winding of each motor carries one-third of the load current, the torque producing currents of MG2, $i_{U(Te)}$, $i_{V(Te)}$, and $i_{W(Te)}$, can be derived from the measured motor currents by

$$\begin{cases} i_{U(Te)} = i_U - (i_A + i_C)/2 \\ i_{W(Te)} = i_W - (i_A + i_C)/2 \\ i_{V(Te)} = -i_{U(Te)} - i_{W(Te)} \end{cases}, \quad (1)$$

where i_U and i_W are measured phrases U and W currents of MG2, and i_A and i_B are measured phrases A and C currents of MG1, respectively. Similarly, the load current can be reconstructed by

$$i_{Load} = 3(i_A + i_C)/2. \quad (2)$$

For mobile power generation, the torque producing currents of MG2, $i_{U(Te)}$, $i_{V(Te)}$, and $i_{W(Te)}$, are projected to the rotor synchronous reference frame as the d and q axis currents, i_{dM} and i_{qM}, through the Clarke and Park transformation using the rotor position information detected by a shaft encoder. Using the field orientation technique and space vector PWM method, the d and q axis currents, i_{dM} and i_{qM}, are controlled through two proportional and integral (PI) controllers with the motor inverter (INV/CONV2) to maintain the inverter dc bus voltage at the commanded level, V^*_{DC}. The other inverter (INV/CONV1) is used to control the load voltage with the help of an inner current loop to improve the dynamic response. The inner current loop is carried out through a high gain proportional controller, while both the dc bus voltage and load voltage are controlled via PI controllers.

To investigate the impact on the efficiency by switching schemes that take the advantages of the unique circuit configurations, the following PWM schemes were used for the inverter, INV1: (1) synchronized switching, in which all three legs switch at the same time, and (2) interleaved switching, in which each phase leg is controlled by its own carrier, whose frequency is one-third of that for the synchronized PWM, and the three carrier signals are phase-shifted by 120 electrical degrees. Due to limitations of the PWM generation hardware in the digital signal processor (DSP) employed in the test set-up, a software implementation of the interleaved PWM based on a single carrier was developed to eliminate the need for external PWM generation logic circuits.

In Fig. 4(b), the system operates in grid support mode using the HV battery as the energy source. Both inverters, INV/CONV1 and INV/CONV2, are used to control the output current. The following combinations of PWM schemes were used for the inverters to assess the impact on the efficiency by the switching schemes: (1) synchronized PWM for both inverters, (2) interleaved PWM for both inverters, and (3) a novel unipolar/interleaved PWM, in which INV/CONV2 is switched at the fundamental frequency while an interleaved PWM is used for INV/CONV1. It is found that the novel unipolar/interleaved PWM scheme can significantly reduce the switching losses while still maintaining a low current distortion factor. Again, the interleaved PWM schemes were implemented using only the built-in PWM hardware designed for three-phase motor control in the DSP.

III. Experimental Results

A prototype electrical drive inverter system was built to test the control schemes. It is comprised of a 55 kW and a 30 kW inverter for the traction motor and generator, respectively, and is configured to provide plug-in charging, mobile generation, and grid support capabilities. Fig. 5 shows a photo of the prototype. The 55 kW inverter was implemented with a 600V/600A six-pack IGBT module, and the 30 kW inverter was implemented with a 600V/300A six-pack IGBT module. The dc bus capacitor bank was constructed using four 375 μF film capacitors rated at 600 V_{DC}. These components are mounted on a 30.48 cm x 17.78 cm water cooled cold plate.

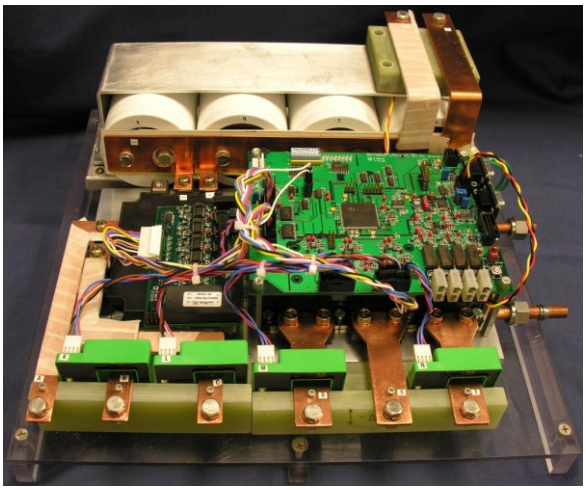

Figure 5. A photo of a traction drive prototype consisting of a 55 kW motor inverter and a 30 kW generator inverter configured for providing plug-in charging and mobile power generation capabilities.

An induction motor of 10.9 kW and a PM motor (used as a generator) rated at 8.2 kW were used in the tests. Table I lists the measured ZS resistances of the motors along with those of the Toyota Camry motors for comparison. Due to the large resistance value of the relatively low power induction motor, the combined ZS resistances of the test motors are quite high at 189.54 mΩ. For comparison, the combined resistance of the two motors in the Camry is 32.32 mΩ, less than 1/5 that of the test motors. This will have a significant impact on the efficiency for the grid support tests.

TABLE I. Measured Motor Zero-Sequence Resistance

	Test Setup	Toyota Camry
Generator	23.8 mΩ	21.58 mΩ
Motor	165.74 mΩ	10.75 mΩ
Combined	189.54 mΩ	32.32 mΩ

The prototype was tested in the mobile generation mode for an output voltage of 120V and in the grid support mode for both 120V and 240V. Fig. 6 illustrates test results showing operating waveforms at output power levels of 3.0 kW and 5.0 kW in the engine-powered generator mode. The near

sinusoidal waveforms of the output voltage and current and a flat DC bus voltage indicate good performance of the controller. Since one-third of the 60 Hz load current is superimposed as a ZS component on the original generator currents, the generator phase currents are no longer sinusoidal.

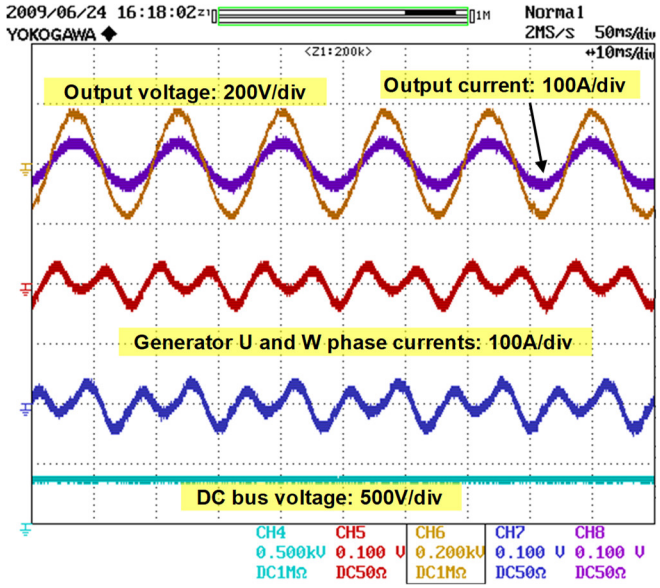

(a) Output power: 3.0 kW at 120V

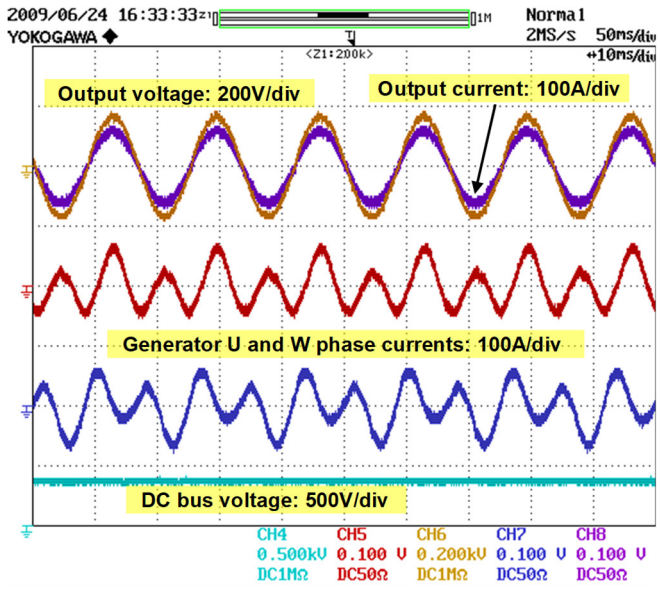

(b) Output power: 5.0 kW at 120V

Figure 6. Typical voltage and current waveforms in the mobile generator mode.

Fig. 7 plots measured total efficiency against output power. Due to the relatively low efficiency (<85%) of the small PM generator, the system efficiency does not exceed 80%. However, it is estimated a maximum efficiency of greater than 90% could be achieved with a production PM generator with efficiency of 93% since the inverter efficiency can reach 97% as will be shown later. In addition, one percentage point improvement is attained with the interleaved switching over the synchronized switching scheme.

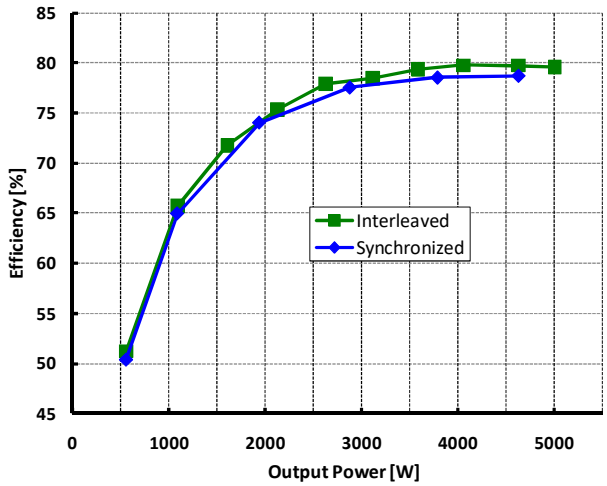

Figure 7. Measured total efficiency in the mobile generator mode.

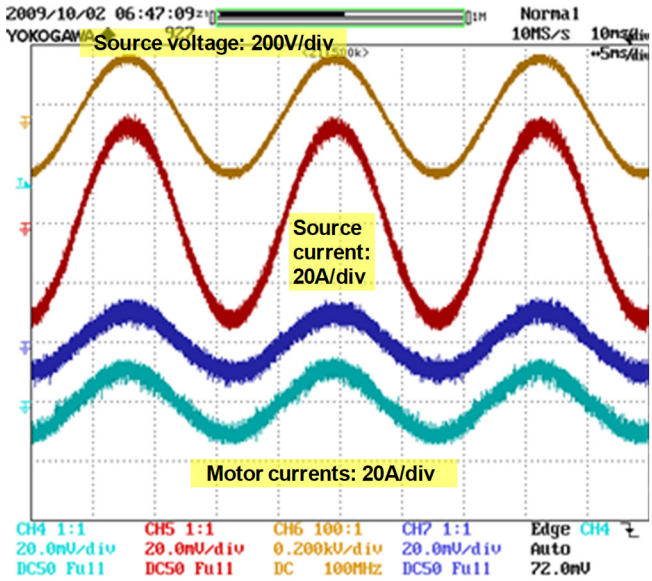

Figure 8. Typical voltage and current waveforms in the grid support mode: supplying power of 3.0 kW at 120V.

Figs. 8 and 9 show operating waveforms in the grid-support mode at the grid (source) voltage of 120V and 240V, respectively. Again, the good sinusoidal output voltage and current waveforms in both cases indicate excellent performance of the control method. In this operation mode, both motors are used as an inductor and one-third of the 60 Hz grid current is flowing in each phase winding as a ZS component, as indicated by the identical two motor phase currents in the test results.

Fig.10 plots measured total efficiency versus output power for the three PWM methods: synchronized, interleaved, and a combination of unipolar and interleaved switching schemes. Estimated efficiency using the resistance values of the Camry motors driven with the proposed novel switching technique is also given to illustrate the impact of the high resistances of the test motors on the efficiency. At the grid voltage of 240V as shown in (a), significant efficiency improvements are achieved with the interleaved over the synchronized switching, and again the interleaved/unipolar switching over

the interleaved PWM scheme, due to the significant reduction of switching losses through the lower switching frequencies in the interleaved/unipolar switching methods. The efficiency improvements are the largest at the beginning since the switching losses are dominant and drop as the output power increases due to the quadratically increasing copper losses at high load current in the high stator resistance of the test motors. It is therefore expected and is indicated by the estimated curve that much better efficiency could be attained at high output power levels with production PM motors whose resistances are much lower than those of the test motors. The maximum measured efficiency is 97.1% at the output power of 6.2kW while the estimated maximum efficiency reaches 98.6%.

Fig. 10(b) shows the measured and estimated total efficiency at the grid voltage of 120V. The measured and estimated maximum efficiencies in this case are 93.7% with an output power of 1.9kW and 95.4% at 2.6kW, respectively.

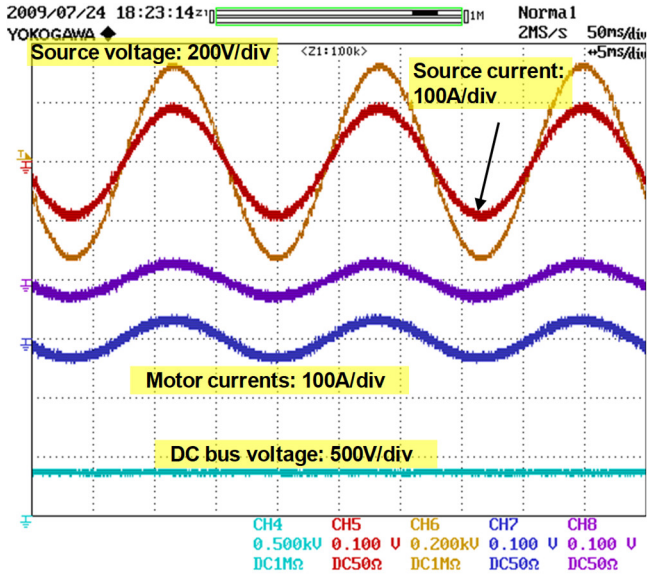

Figure 9. Typical voltage and current waveforms in the grid support mode: supplying power of 14.7 kW at the grid voltage of 240V.

IV. CONCLUSIONS

Using the onboard electrical drive systems in HEVs to provide plug-in charging capability offers many benefits, including (1) significantly reducing the cost and volume of battery chargers for PHEVs, (2) providing rapid charging capability, and (3) enabling the use of the PHEVs as mobile generators and grid support energy storage devices. In this paper, PWM switching schemes uniquely suited for control of this type of PHEVs for mobile power generation and grid support applications are proposed and examined experimentally. In particular, it is found a novel unipolar/ interleaved PWM switching scheme can significantly reduce the switching losses and substantially increase the efficiency.

ACKNOWLEDGMENT

The authors thank Mr. Cliff White for his assistance in assembling the hardware test setup.

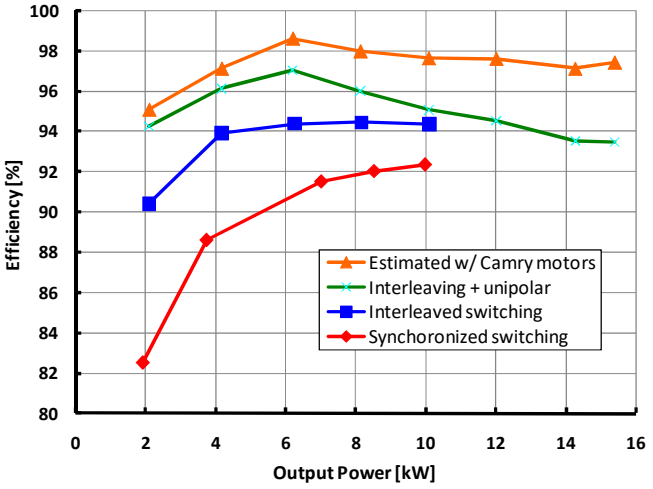

(a) At grid voltage of 240V

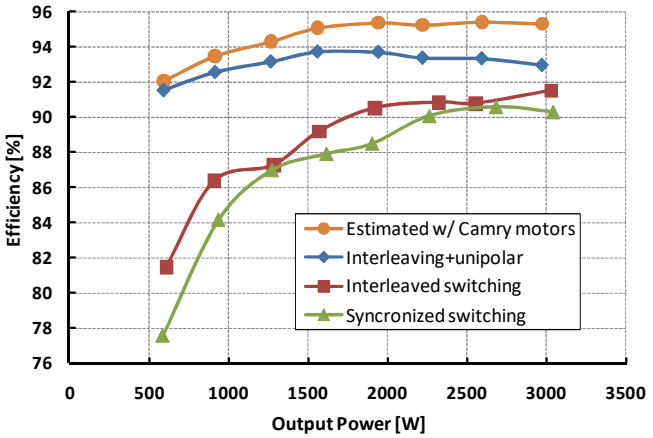

(b) At grid voltage of 120V

Figure 10. Measured and estimated total efficiency in the grid support mode.

REFERENCES

[1] U.S. Department of Energy, "HEV Sales by Model – Trend of sales by HEV models from 1999-2008," http://www.afdc.energy.gov/afdc/data/docs/hev_sales.xls.

[2] Toyota Motor Corporation, "Sustainability Report 2008," http://www.toyota.co.jp/en/csr/report/08/download/index.html.

[3] The California Cars Initiative (CalCars.org), "Plug-In Hybrids: State Of Play, History & Players," http://www.calcars.org/history.html.

[4] U.S. Dept. of Energy, "Plug-In Hybrid Electric Vehicle Benefits," http://www.afdc.energy.gov/afdc/vehicles/plugin_hybrids_benefits.html.

[5] D. Thimmesch, "An SCR inverter with an integral battery charger for electric vehicles," IEEE Trans. on Industry Applications, vol. IA-21, no. 4, pp.1023–1029, Jul./Aug. 1985.

[6] S.-K. Sul and S.J. Lee, "An integral battery charger for four-wheel drive electric vehicle", IEEE Transactions on Industry Applications, vol. 31, no. 5, pp. 1096–1099, Sept./Oct. 1995.

[7] T. Ishikawa, T. Sekimori and Y. Hotta, "Development of a Traction Inverter with Charging Function", EVS-14, Orlando, FL, Dec. 11–17, 1997.

[8] L. Tang and G.J. Su, "A Low-Cost, Digital-Controlled Charger for Plug-In Hybrid Electric Vehicles," in IEEE Energy Conversion Conference & Exposition (ECCE), Sept. 20-24, 2009, San Jose, CA, pp. 3923–3929.

[9] H. Oyobe, M. Nakamura, T. Ishikawa, S. Sasaki, Y. Minezawa, Y. Watanabe, and K. Asano, "Development of ultra low-cost, high-capacity power generation system using drive motor and inverter for hybrid vehicle," in IEEE 40th IAS Annual Meeting, 2005, vol. 3, pp. 2029–2034.